Front. Electr. Electron. Eng. China 2010, 5(2): 128–136
DOI 10.1007/s11460-010-0017-y

RESEARCH ARTICLE

Ying CAO, Xin HAO, Xiaoen ZHU, Shunren XIA

An adaptive region growing algorithm for breast masses in mammograms

Abstract This study attempted to accurately segment the mammographic masses and distinguish malignant from benign tumors. An adaptive region growing algorithm with hybrid assessment function combined with maximum likelihood analysis and maximum gradient analysis was developed in this paper. In order to accommodate different situations of masses, the likelihood and the edge gradients of segmented masses were weighted adaptively by the use of information entropy. 106 benign and 110 malignant tumors were included in this study. We found that the proposed algorithm obtained segmentation contour more accurately and delineated the tumor body as well as tumor peripheral regions covering typical mass boundaries and some spiculation patterns. Then the segmented results were evaluated by the classification accuracy. 42 features including age, intensity, shape and texture were extracted from each segmented mass and support vector machine (SVM) was used as a classifier. The classification accuracy was evaluated using the area (A_z) under the receiver operating characteristic (ROC) curve. It was found that the maximum likelihood analysis achieved an A_z value of 0.835, the maximum gradient analysis got an A_z value of 0.932 and the hybrid assessment function performed the best classification result where the value of A_z was 0.948. In addition, compared with traditional region growing algorithm, our proposed algorithm is more adaptive and provides a better performance for future works.

Keywords mass lesion segmentation, adaptive region growing algorithm, maximum likelihood analysis, information entropy, support vector machine (SVM)

Received January 29, 2010; accepted March 1, 2010

Ying CAO, Xin HAO, Xiaoen ZHU, Shunren XIA (✉)
Key Laboratory of Biomedical Engineering of Ministry of Education, Zhejiang University, Hangzhou 310027, China
E-mail: srxia@zju.edu.cn

1 Introduction

Breast cancer is among the leading causes of death in women [1]. The early diagnosis and treatment can significantly increase the patients' survival chance [2–4]. Computer-aided diagnosis (CAD) system was developed to assist radiologists in mammographic mass detection and diagnosis [5,6].

Mass lesion segmentation, which extracts the mass from the surrounding tissues, is an essential step in the computerized analysis of mammograms. Because mass lesions are usually embedded and hidden in varying densities of parenchymal structures, the task of mass segmentation is not trivial. A large number of studies have been conducted in an attempt to improve the performance of CAD in mass segmentation [7]. Several experts exploited the methods using intensity value as the global or local threshold to decide if a pixel should be placed in the region of interest (ROI) or background [8,9]. Reference [10] used a filtering method called the density weighted contrast enhancement (DWCE) method to segment masses. Reference [11] proposed a *K*-means clustering algorithm which includes spatial constraints and accounting for local intensity variations to extract the mass regions.

Most of these methods are successful at segmenting the circumscribed masses with high contrast. However, the accurate boundaries of masses with ill-defined edges and adhesion tissues cannot be properly obtained. Conventional region growing is an effective pixel-based segmentation method and is robust to tissue interference. Reference [12] has used the region growing process, which is restricted by Canny edge detection, to obtain a better segmentation performance over the conventional methods. The region growing algorithm can produce an accurate mass contour if a suitable threshold is chosen. Thus, setting optimal threshold automatically becomes the most important task in improving this algorithm. Previous research has been reported to use multiple threshold values to get many growing contours per mammographic image and use maximum likelihood analysis to determine the optimal threshold for region growing [13]. However, this method is only based on probability assessment of mass region and will produce an over-segmentation result if there is no obvious boundary or high contrast between the adhesion tissue and tumor region. Hence, it is impossible for maximum likelihood analysis itself to determine the proper threshold of all mammographic images.

For the reasons above, a hybrid assessment function considering both the likelihood and the edge gradients of segmented masses is developed. In order to accommodate the different situations of masses, these two components are adaptively weighted by using the information entropy of the segmented image. Then, the best mass contour will be selected by this hybrid assessment function.

Segmentation is the basis of the separation for the benign and malignant tumors and more accurate segmentation results represent the better classification accuracy. In order to evaluate the performance of segmented results, a group of features is extracted from the segmented masses and support vector machine (SVM) is used as a classifier for the classification of mammographic masses. Then receiver operating characteristic (ROC) analysis is applied to evaluate the performance of the classification.

The organization of this paper is as follows: The details of the methods for breast masses, including the image enhancement approach, the adaptive segmentation algorithm and the classification, are given in Sect. 2. The database, segmentation results and classification results of mammographic masses are discussed in Sect. 3. The conclusions are drawn in Sect. 4.

2 Methods

Figure 1 presents the flowchart of our method for breast masses in mammograms. It involves three major stages: image enhancement, mass segmentation and performance evaluation. In this study, the masses were segmented by the adaptive region growing algorithm and then the segmented results are evaluated by the classification accuracy.

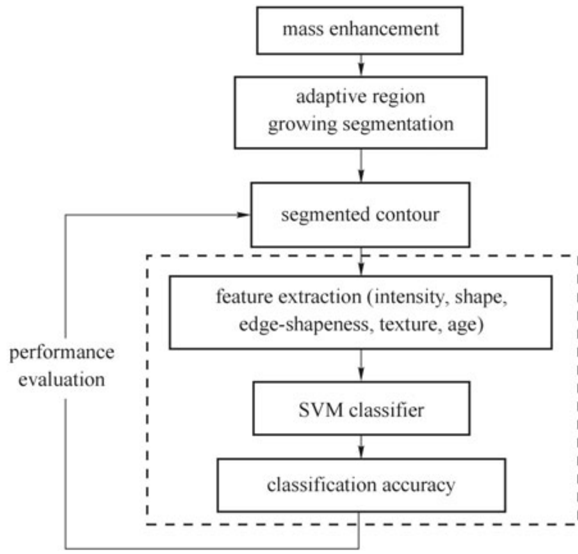

Fig. 1 Flowchart of breast mass segmentation scheme

2.1 Image enhancement

In order to enhance the contrast and reduce the ambiguity of mammographic images, image enhancement is a necessary process before segmentation. Single fuzzy enhancement approach was first used to improve the contrast between tumor region and background [14]. Then a multi-scale enhancement approach was used to reduce noise and strengthen the edge [15].

As widely used in the image enhancement, the fuzzy set theory can provide a suitable way in analyzing the images with ambiguous edges. The single fuzzy enhancement approach starts with the transformation of gray level and then a fuzzy set is obtained. A certain threshold is used to divide the fuzzy set into two parts and these two parts of fuzzy set are processed for contrast enhancement respectively. The details of this algorithm can be found in Ref. [14].

Multi-scale analysis represents the local mammographic features and has the ability to emphasize mammographic features while suppressing the noise. In this enhancement approach, discrete wavelet transform (DWT) is performed on the image, each wavelet coefficient of every detail subband is then suppressed and only the coefficients that are larger than a certain threshold are enhanced. Therefore, the pixels on the edge will be enhanced while the background noise will be reduced at the same time. The details of this algorithm can be found in Ref. [15].

2.2 Mass segmentation

2.2.1 Region growing

Region growing is an automatic segmentation method in which the segmentation region begins as a single pixel and grows based on surrounding pixels with similar properties, e.g., gray-scale level or texture. Typically, the seed is located in the center region with the highest intensity in the suspected region. The next 4-neighboring or 8-neighboring pixel is checked for similarity so that the region can grow. In our algorithm, the 4-neighboring pixel of the seed pixel is checked and a gray level threshold is used for the similar criteria. If a 4-neighboring of a pixel has a gray value smaller than or equal to the threshold, it is included in the region of interest. The neighboring pixels in the alternate direction are swept until no more pixels are acquired in the sweeping step [16]. The segmented region can be grown by repeating the same method with a different threshold. The higher the intensity threshold is, the larger the contour we can obtain.

2.2.2 Maximum likelihood analysis

In order to select an optimal threshold for region growing automatically, Ref. [13] proposed a method to add a maximum likelihood component to the region growing algorithm. This algorithm is given as follows: First, by using the same seed point with multiple intensity threshold values, a sequence of growing contours is obtained per lesion. Then the composite probability P_i for each segmented region S_i is calculated:

$$P_i = p((S_i)_{\text{foreground}}|\text{PDF}_i)p((S_i)_{\text{background}}|\text{ROI}), \qquad (1)$$

where $p((S_i)_{\text{foreground}}|\text{PDF}_i)$ is the probability density function (PDF) of the segmented region and $p((S_i)_{\text{background}}|\text{ROI})$ is the PDF of background. The PDF is calculated inside the contour, S_i, where i is the threshold step. Then the logarithm of the composite probability is calculated in the following way:

$$\lg P_i = \lg p((S_i)_{\text{foreground}}|\text{PDF}_i) + \lg p((S_i)_{\text{background}}|\text{ROI}). \qquad (2)$$

The likelihood that the contour represents the accurate borders of mass is determined by assessing the maximum change of the likelihood function:

$$\arg\max \frac{\mathrm{d}\lg P_i}{\mathrm{d}i}. \qquad (3)$$

To summarize, the best contour is determined by locating the steepest jump in likelihood values, i.e., the intensity threshold corresponding to this location will produce the best contour.

Maximum likelihood analysis is able to perform a good segmentation result on the mammographic image with blurred edge and high contrast while it will produce a problem of over-segmentation if there are adhesion tissues surrounding the mass.

2.2.3 Adaptive region growing algorithm

1) Maximum gradient analysis

Edge information of the image is generally carried out by computing the gradient which is corresponding to the significant change of the image gray value. Compared with the smooth region, the gradients on the edge of the mass will have a higher value. Therefore, the segmented contour with maximum average gradient is considered to be closest to the exact edge. In this algorithm, the average gradients of the edges are also used to assess the best segmented contour as the maximum likelihood analysis.

The processing steps of maximum gradient analysis are similar to the maximum likelihood analysis. To begin with, by using the same seed point with multiple intensity threshold values, a sequence of growing contours is obtained per lesion. Then a series of the edge average gradients $\overline{g_i}$ are calculated and the gradient assessment function is calculated as follows:

$$\arg\max \overline{g_i}. \qquad (4)$$

To summarize, Eq. (4) intends to find the maximum value of the aforementioned gradient values as a function of intensity threshold. The intensity value corresponding to this maximum gradient value is assessed to be the optimal threshold for mass segmentation. Then the best segmented contour is obtained corresponding to this optimal threshold.

The maximum gradient analysis can overcome the interference of adhesion tissue and get a better segmented result if the mass has an obvious edge. However, due to the existence of blurred edge, the image will be ill-segmented by using this method.

2) Hybrid assessment function

As we mentioned above, the maximum likelihood analysis and the maximum gradient analysis suit different situations of the images, which are quite complementary to each other. Therefore, the innovation of this proposed algorithm is emphasized on the combination of the likelihood component and the edge gradient component. Moreover, in order to accommodate different masses, the weights of these two components are adaptively adjusted. Information entropy is a common concept in the information theory and is frequently used to measure the amount of information. The more orderly a system is, the lower information entropy it will have. The goal of the mass segmentation is to classify the ROI into mass region and background. The better classification result shows that there is lower uncertainty of classification and the system is more orderly, which means a lower value of information entropy.

The hybrid algorithm is summarized as follows: first of all, the maximum likelihood analysis and the maximum gradient analysis are carried out respectively and two optimal thresholds T_{L} and T_{G} are obtained. Taking T_{L} as an example, the mass region and background are segmented by using the T_{L} and two probability distributions of gray level are expressed by $p_0, p_1,..., p_T$ and $p_{T+1}, p_{T+2},..., p_n$. In this study, the entropy is defined as follows:

$$H = -\sum_{i=1}^{m} p_i \lg p_i, \qquad (5)$$

where p_i is the probability of gray-scale. Next, the information entropies of these two distributions are calculated respectively and the sum of entropies is expressed as follows:

$$\begin{aligned} H_{\mathrm{L}} &= H_{\text{foreground}} + H_{\text{background}} \\ &= -\sum_{i=T+1}^{n} p_i \lg p_i - \sum_{i=1}^{T} p_i \lg p_i. \end{aligned} \qquad (6)$$

H_G is calculated in the same way. It is observed that better segmentation result shows lower value of H. Using H_L and H_G as the weights for the likelihood component and the edge gradient component separately, the hybrid assessment function is given.

$$\arg\max\left[(\mathrm{e}^{H_G})^{\alpha}\frac{\mathrm{d}\,\lg P_i}{\mathrm{d}i}+(\mathrm{e}^{H_L})^{\alpha}\overline{g_i}\right]. \tag{7}$$

$\mathrm{d}\,\lg P_i/\mathrm{d}i$ and $\overline{g_i}$ need to be normalized before Eq. (7) is calculated. In order to ensure that the weights are always positive, the entropy value H is transformed into $(\mathrm{e}^{H})^{\alpha}$ and α is used to reduce the gap between the two weights. It is found that when H_L is smaller than H_G, which means that the assessment result based on the maximum likelihood analysis is better than the maximum gradient analysis, $(\mathrm{e}^{H_G})^{\alpha}$ is bigger than $(\mathrm{e}^{H_L})^{\alpha}$ and the assessment component of likelihood will obtain a higher weight. Then it will play a greater role in assessing the best contour.

2.3 Performance evaluation

2.3.1 Feature extracting

One extremely important task in the separation of malignant and benign tumors is feature selection and calculation. Benign tumors can be lucent at the center and can have well-defined borders, while malignant tumors can have speculated and/or fuzzy borders. In total, 42 features were extracted from each segmented ROI including the patient age, five intensity features (Ct, Co, AG, Sk, Ku), two edge-sharpness features (A, Ev), six shape features (SI, FC, FD, FF, C and Area) and 28 texture features, which are explained in the following paragraphs.

1) Patient age

Patient age is a feature that can be collected conveniently and has been included in CAD systems by several groups [17,18]. In this paper the age is also used as one type of features.

2) Intensity features

Most of the intensity features are the simple statistics. Five intensity features are considered in this study [19], including contrast (Ct), coherence (Co), average gray level of ROI (AG), skewness (Sk) and kurtosis (Ku). The feature Ct is the contrast measure of the suspicious region. Generally, it is different between the average gray level of the ROI and the average gray level of the surrounding region. The other four features are the statistics pertinent to the moments.

3) Edge-sharpness features

Two edge-sharpness features are used in this study, including acutance (A) and variation coefficient of the edge (Ev). A is a measure of the sharpness or change in density across a mass margin [20]. Ev is a measure of the edge contrast.

4) Shape features

Six shape features are considered in this study, including speculation index (SI), fractional concavity (FC), fractal dimension (FD), Fourier factor (FF), compactness (C) and area (Area). SI represents the degree of spiculation of the contour. Reference [21] proposed an algorithm to compute SI based upon a polygonal model of the given contour and a combination of the segment lengths, base widths, and angles of possible spicules. Because of their effect on the surrounding tissues, most malignant tumors from narrow, stellate distortions around their boundaries and, hence, have higher values of SI than benign masses with smooth contours. FD is used to measure the complexity, irregularity, or space-filling nature of the contour and is derived by using the two-dimensional ruler method [22]. FF is a measure related to the presence of roughness in terms of high-frequency component in the contours. Contours of malignant tumors are expected to be rougher, in general, than the contours of benign masses; hence, the FF value is expected to be higher for the former than the latter [21]. C is a simple measure of the efficiency of a contour enclosing a given area. A high compactness value indicates a large perimeter enclosing a small area. Typically benign masses may be expected to have lower values of compactness as compared to typically malignant tumors [21,22].

5) Texture features

13 texture features are computed according to the definition of gray level co-occurrence matrix (GLCM) by Ref. [23] and 15 texture features are derived from the gradient gray level co-occurrence matrix (GGCM) [24]. A ribbon of pixels around the segmented margin of each mass is used to compute texture features. The width of the ribbon is 8 mm and the ribbon is obtained by dilating the mass boundaries after filtering and down-sampling the mammograms to an effective resolution. The texture features derived from GLCM includes the angular second moment (f_1), correlation degree (f_2), entropy (f_3), contrast (f_4), inverse difference moment (f_5), sum average (f_6), sum entropy (f_7) , sum variance (f_8), variance (f_9), difference average (f_{10}), inertia (f_{11}), difference variance (f_{12}), and difference entropy (f_{13}). The other group of texture features derived from GGCM includes low gradient advantage (g_1), high gradient advantage (g_2), the uneven distribution of gray (g_3), the uneven distribution of gradient (g_4), energy (g_5), average gray (g_6), average gradient (g_7), gray-scale mean-variance (g_8), gradient scale mean-variance (g_9), coherence (g_{10}), gray entropy (g_{11}), gradient entropy (g_{12}), hybrid entropy (g_{13}), inertia (g_{14}), and inverse difference moment (g_{15}).

2.3.2 Classification

Another extremely important task in the separation of malignant and benign tumors is choosing an optimal classification method. Machine learning methods have been demonstrated to generate very good results in classification. The SVM, which is introduced by Ref. [25] in 1995, is a method to estimate the function classifying the data into two classes and is applied in this paper for classification. The basic idea of SVM is to construct a hyper plane as the decision surface in such a way that the margin of separation between benign and malignant examples is maximized. The SVM term comes from the fact that the points in the training set that are closest to the decision surface are called support vectors. SVM achieves this by the structural risk minimization principle that is based on the fact that the error rate of a learning machine on the test data is bounded by the sum of the training-error rate and a term that depends on the Vapnik-Chervonenkis (VC) dimension. The details of this algorithm can be found in Refs. [26–28].

The performance of the classification results are evaluated with ROC analysis using the LABROC program [29] and the area under the ROC curve, A_z, is used to measure the classification accuracy.

3 Results

3.1 Database

The images used in the study were randomly selected from a publicly available database, the digital database for screening mammography (DDSM), assembled by a research group at the University of South Florida [30]. The database provides high-resolution digitized film screen mammograms which are scanned at a sampling rate of 42–50 mm and either 12 or 16 bits per pixel. In the DDSM, a total of 1000 diagnosed masses are extracted using the provided ground truth annotations. In particular, a square crop centered on the location of each annotated mass is selected. The size was chosen so that the ratio between the crop area and the area of the annotated mass is nearly 1.2. The range of image pixel gray level was also compressed from 12 to 8 bits. 106 benign and 110 malignant mass samples were selected in this study.

Each mass on each mammographic view has assessment information which is specified by an experienced radiologist. The assessment code is a value from one to five, and comes from the American College of Radiology (ACR) breast imaging reporting and data system (Bi-RADS) [31] standard. Figure 2(a) shows the distribution of the malignancy ranking of the masses. The grade of the ranking is divided into 5: 1, negative; 2, benign; 3, probably benign; 4, suspicious abnormality, and 5, highly suggestive of malignancy. As expected from the fact that all cases underwent biopsy, the two distributions partially overlap. Figure 2(b) shows the distributions of the size of the malignant and benign masses. The size was measured as the longest dimension of the lesion by the radiologist. It ranged from 10 to 50 mm with a mean size of 35 mm. The distributions of the size of malignant and benign tumors are similar to each other.

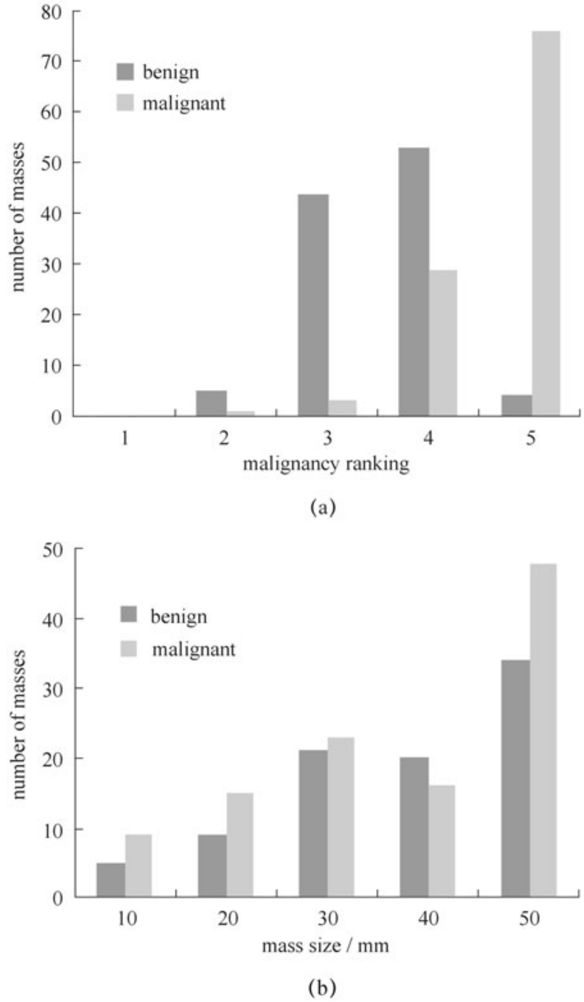

Fig. 2 Information distributions provided in DDSM for our data set. (a) Distribution of malignancy ranking; (b) distribution of mass size

3.2 Segmentation

In our numerical experiments, the parameters of the proposed methods were chosen as follows: the image gray values were normalized between 0 and 1. $\alpha = 0.1$. Taking into account the distribution of gray-scale of masses, the scope of multiple thresholds was set between 0.2 and 0.8 and the stepping threshold interval was 0.012.

Figure 3(a) shows an ROI of a clinical case containing a typical example of ill-defined and blurred lesion margin. As the images shown in Figs. 3(b)–3(e), the edge gradient information of the original image is not very obvious, but after the preprocessing of single fuzzy enhancement and wavelet enhancement, both the contrast and the edge of the image are strengthened and the noise is reduced. Figure 3(i)

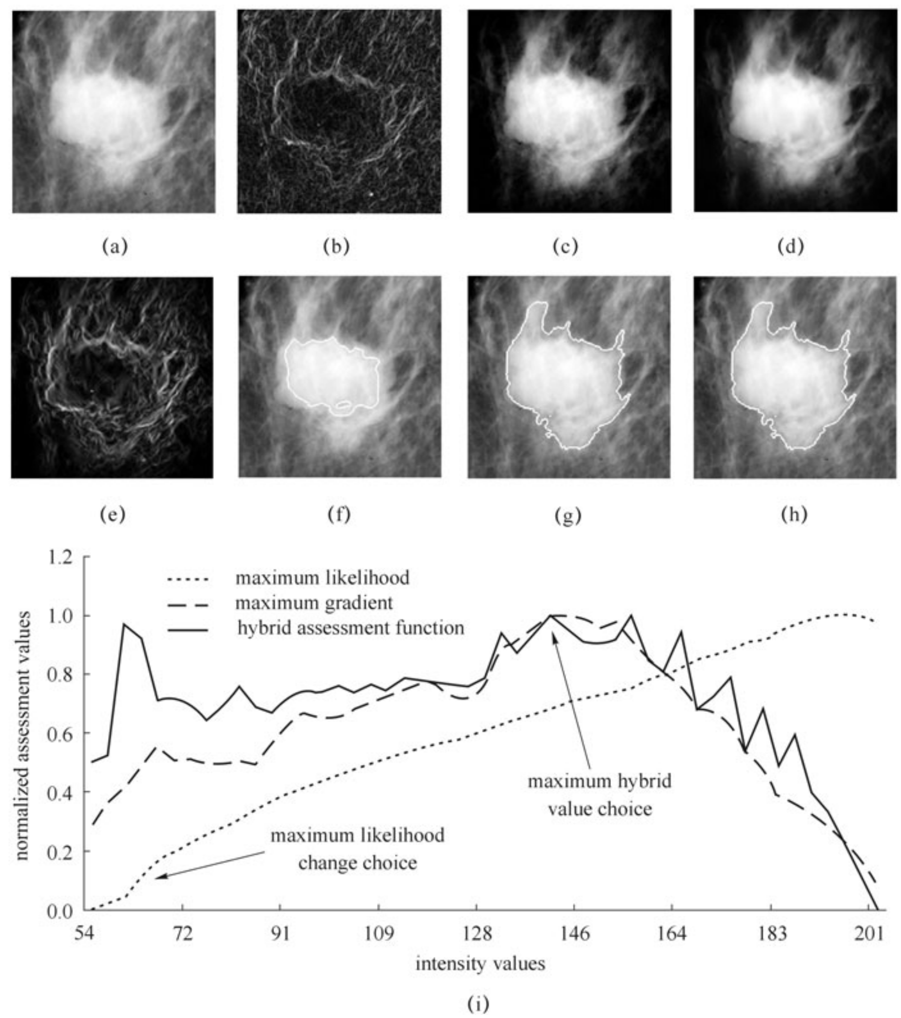

Fig. 3 Results for an exemplary clinical case containing a benign breast lesion. (a) Original image; (b) gradient of original image; (c) image preprocessed by single fuzzy enhancement; (d) image preprocessed by wavelet transform; (e) gradient of enhancement image; (f) segmentation result by maximum likelihood analysis; (g) segmentation result by maximum gradient analysis; (h) segmentation result by hybrid assessment function; (i) plot of three different assessment functions with respect to threshold values for all segmentation steps

shows the plot of three different assessment functions with respect to threshold values. In the maximum likelihood analysis, the steepest jump location, where the arrow points to in dot-line (in Fig. 3(i)), illustrated maximum likelihood change choice and the correlative threshold corresponding to this algorithm was selected. Similarly, the threshold corresponding to the maximum hybrid value was chosen by the hybrid assessment function. (In this case, the same point was both selected by the maximum gradient analysis and the hybrid method. Therefore, the same threshold was chosen by these two methods.) The segmentation results of these two methods are shown in Figs. 3(f) and 3(h). It is observed that the maximum likelihood analysis failed due to the uneven distribution of gray-scale in the mass region. However, using maximum gradient analysis for assessing the best contour could overcome this ill-segmentation problem. The hybrid assessment function chooses the higher threshold by using the weights of information entropy and obtained an accurate boundary, which is the same with maximum gradient analysis.

Figure 4 illustrates the other four typical lesion examples using these three assessment methods. The original images are illustrated in Fig. 4(a). Figure 4(b) shows the segmented results of maximum likelihood analysis. From these four images, we can see that if the mass has a clear edge without any adherent tissue or the gray-scale contrast between the mass and the background is high, the maximum likelihood analysis can get a perfect segmented result. However, if the mass has a blurred edge or the contrast is low, the result would be ill-segmented or over-segmented. No matter what the gray-scale contrast is, the algorithm of maximum gradient can also get a better segmented result as long as the mass has a strong edge gradient value. However, if the gradient values cannot accurately perform the edge or the distribution of gradient

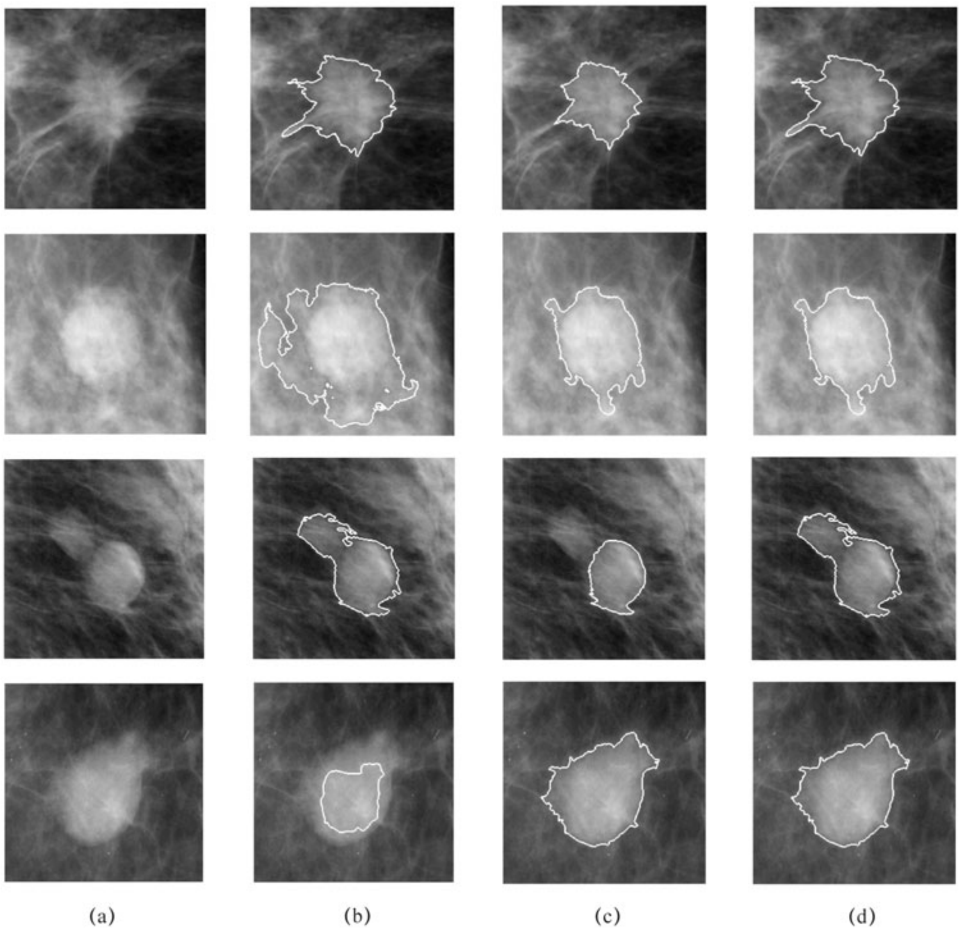

Fig. 4 Segmentation results for four lesion examples. (a) Original images; (b) segmented results based on maximum likelihood analysis; (c) segmented results based on maximum gradient analysis; (d) segmented results based on hybrid assessment function

value is uneven along the mass margin, the segmented results should be poor performance. The segmented results of this method are given in Fig. 4(c). Figure 4(d) shows the segmented results based on the hybrid assessment function. Compared with the results in Fig. 4(b) and Fig. 4(d), the proposed method, which overcomes the problem of ill-segmentation and over-segmentation, is more adaptive and robust.

3.3 Classification accuracy

The 106 benign and 110 malignant mass tumors, which were segmented based on the above segmentation algorithms, were tested in the classification method. All the features extracted from these segmented mass tumors were then put into the SVM classifier. 53 benign and 55 malignant mass tumors were randomly selected as the training samples and the remaining tumors were used as the predicted samples. Finally, ROC is used to measure the classification accuracy of these predicted samples.

Figure 5 shows the classification accuracy of the three segmentation algorithms. It can be found that the hybrid assessment function performs the best classification result ($A_z = 0.948$), and the method of maximum gradient has the next best performance ($A_z = 0.932$). The maximum likelihood performs worst and the A_z value is 0.835. As can be seen from Fig. 5, the classification results are in agreement with the segmented results and the adaptive region growing algorithm can perform a better result for the future work.

4 Discussion and conclusions

In this paper, a novel segmentation algorithm based on adaptive region growing is proposed. The main contribution of this algorithm is that a hybrid assessment function combined with the maximum likelihood analysis and the maximum gradient analysis is developed and the weights of these two components are self-adaptively adjusted by using the information entropy of the segmented image. In our studies, the method of the maximum likelihood analysis is effective for segmenting the masses with blurred edge and the maximum gradient analysis is good at

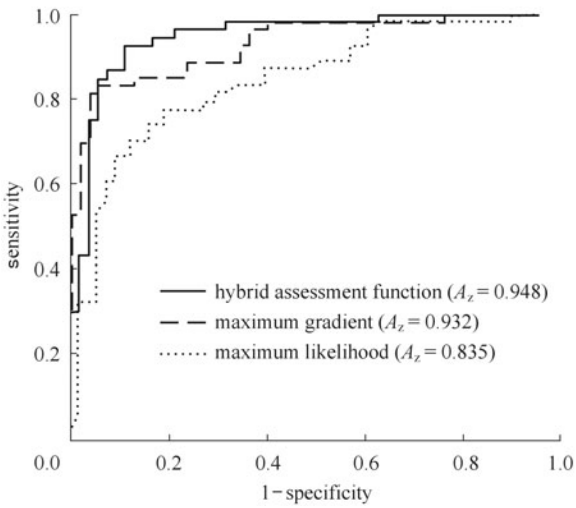

Fig. 5 ROC curves for SVM classification result

overcoming the interference of adhesion tissue. The role of this hybrid assessment function is to choose a better segmentation method between these two analysis functions and it is confirmed by the classification results.

As we have known, the information entropy is such a parameter implying the uncertainty between mass region and background that is chosen to evaluate the effect in image segmentation. In this hybrid assessment function, it plays a crucial and inversely proportional role in adjusting the weights of the two analysis functions. Hence, the following two cases may make this function disabled. One case is that high information entropy may lead to an auto-misjudgment of the two weights on the condition that the background is accompanied with a great amount of surrounding tissues, or uneven gray-scale distribution of mass region occurs. Another case is that neither of the two analysis functions is effective as long as the uneven gray-scale distribution occurs synchronously with weak edge gradient information. In both cases, further image enhancement for strengthening the edge and reducing the interference from the surrounding tissues is extremely imperative. Another aspect of defect is that not all of the features extracted from the image can perform a good classification result. Meanwhile the combination of different features will also show effects.

This proposed adaptive region growing algorithm has wide applications in segmenting most gray images, especially with only one target region. Despite the limitation of this proposed method, the hybrid assessment function should be proposed because of its high robustness and adaptability. The segmented result with this algorithm provides a good performance for future works. Potential improvements may be achieved by including additional image features and selecting an appropriate combined feature space for classification.

Acknowledgements This work was supported by the National Natural Science Foundation of China (Grant No. 60772092).

References

1. Mettlin C. Global breast cancer mortality statistics. CA: A Cancer Journal for Clinicians, 1999, 49(3): 138–144
2. Miller A B. Mammography: reviewing the evidence. Epidemiology aspect. Canadian Family Physician, 1993, 39: 85–90
3. Smart C R, Hendrick R E, Rutledge J H 3rd, Smith R A. Benefit of mammography screening in women ages 40 to 49 years: current evidence from randomized controlled trials. Cancer, 1995, 75(7): 1619–1626
4. Hao X, Cao Y, Xia S R. Computer-aided diagnosis technique on mammograms using content-based medical image retrieval. Chinese Journal of Biomedical Engineering, 2009, 28(6): 922–930 (in Chinese)
5. Tang J S, Rangayyan R M, Xu J, EI Naqa I, Yang Y Y. Computer-aided detection and diagnosis of breast cancer with mammography: recent advances. IEEE Transactions on Information on Technology in Biomedicine, 2009, 13(2): 236–251
6. Shen Y, Xia S R, Li M D. A survey on relevance feedback techniques in content based medical image retrieval. Chinese Journal of Biomedical Engineering, 2009, 28(1): 128–136 (in Chinese)
7. Cheng H D, Shi X J, Min R, Hu L M, Cai X P, Du H N. Approaches for automated detection and classification of masses in mammograms. Pattern Recognition, 2006, 39(4): 646–668
8. Brzakovic D, Luo X M, Brzakovic P. An approach to automated detection of tumors in mammograms. IEEE Transactions on Medical Imaging, 1990, 9(3): 233–241
9. Li L, Qian W, Clarke L P, Clark R A, Thomas C J. Improving mass detection by adaptive and multi-scale processing in digitized mammograms. Proceedings of SPIE, 1999, 3661: 490–498
10. Petrick N, Chan H P, Sahiner B, Wei D, Helvie M A, Goodsitt M M, Adler D D. Automated detection of breast masses on digital mammograms using adaptive density-weighted contrast-enhancement filtering. Proceedings of SPIE, 1995, 2434: 590–597
11. Pappas T N. An adaptive clustering algorithm for image segmentation. IEEE Transactions on Signal Processing, 1992, 40(4): 901–914
12. Xu W D, Xia S R, Duan H L, Xiao M. Segmentation of mass in mammograms using a novel intelligent algorithm. International Journal of Pattern Recognition and Artificial Intelligence, 2006, 20 (2): 255–270
13. Kinnard L M, Lo S B, Wang P C, Freedman M T, Chouikha M F. Separation of malignant and benign masses using maximum-likelihood modeling and neural networks. Proceedings of SPIE, 2002, 4684: 733–741
14. Pal S K, King R A. Image enhancement using fuzzy set. Electronics Letters, 1980, 16(10): 376–378
15. Laine A F, Schuler S, Fan J, Huda W. Mammographic feature enhancement by multiscale analysis. IEEE Transactions on Medical Imaging, 1994, 13(4): 725–740
16. Kinnard L, Lo S C B, Wang P, Freedman M T, Chouikha M F. Automatic segmentation of mammographic masses using fuzzy

shadow and maximum-likelihood analysis. In: Proceedings of IEEE International Symposium on Biomedical Imaging. 2002, 241–244
17. Kallergi M. Computer-aided diagnosis of mammographic microcalcification clusters. Medical Physics, 2004, 31(2): 314–326
18. Jesneck J L, Nolte L W, Baker J A, Floyd C E, Lo J Y. Optimized approach to decision fusion of heterogeneous data for breast cancer diagnosis. Medical Physics, 2006, 33(8): 2945–2954
19. Mavroforakis M E, Georgiou H V, Dimitropoulos N, Cavouras D, Theodoridis S. Mammographic masses characterization based on localized texture and dataset fractal analysis using linear, neural and support vector machine classifiers. Artificial Intelligence in Medicine, 2006, 37(2): 145–162
20. Rangayyan R M, EI-Faramawy N M, Desautels J E L, Alim O A. Measures of acutance and shape for classification of breast tumors. IEEE Transactions on Medical Imaging, 1997, 16(6): 799–810
21. Rangayyan R M, Nguyen T M. Fractal analysis of contours of breast masses in mammograms. Journal of Digital Imaging, 2007, 20(3): 223–237
22. Rangayyan R M, Nguyen T M. Pattern classification of breast masses via fractal analysis of their contours. International Congress Series, 2005, 1281(4): 1041–1046
23. Haralick R M, Shanmugam K, Dinstein I. Textural features for image classification. IEEE Transactions on Systems, Man, and Cybernetics, 1973, SMC-3(6): 610–621
24. Zhou M Q, Geng G H, Wei N. Content-Based Image Retrieval. Beijing: Tsinghua University Press, 2007 (in Chinese)
25. Vapnik V N. The Nature of Statistical Learning Theory. New York: Springer-Verlag, 1995
26. Campanini R, Dongiovanni D, Iampieri E, Lanconelli N, Masotti M, Palermo G, Riccardi A, Roffilli M. A novel featureless approach to mass detection in digital mammograms based on support vector machines. Physics in Medicine and Biology, 2004, 49(6): 961–975
27. Mu T, Nandi A K, Rangayyan R M. Classification of breast masses using selected shape, edge-sharpness, and texture features with linear and kernel-based classifiers. Journal of Digital Imaging, 2008, 21(2): 153–169
28. Yu S, Yang X W, Hao Z F, Liang Y C. An adaptive support vector machine learning algorithm for large classification problem. Lecture Notes in Computer Science, 2006, 3971: 981–990
29. Metz C E, Herman B A, Shen J H. Maximum likelihood estimation of receiver operating characteristic (ROC) curves from continuously-distributed data. Statistics in Medicine, 1998, 17(9): 1033–1053
30. Heath M, Bowyer K, Kopans D, Moore R, Kegelmeyer P. The digital database for screening mammography. In: Proceedings of the 5th International Workshop on Digital Mammography. 2000, 212–218
31. American College of Radiology (ACR). Breast imaging reporting and data system atlas (BI-RADS atlas). Reston: American College of Radiology, 2003